Hydrogen Bond Breaking and Reformation in Alcohol Oligomers Following Vibrational Relaxation of a Non-Hydrogen-Bond Donating Hydroxyl Stretch

K. J. Gaffney, I. R. Piletic, and M. D. Fayer*

Department of Chemistry, Stanford University, Stanford, California 94305

Received: May 9, 2002; In Final Form: August 12, 2002

Vibrational relaxation in methanol-*d*, ethanol-*d*, and 1-propanol-*d* dissolved in CCl_4 has been measured with ultrafast infrared pump−probe experiments. Non-hydrogen-bond donating OD stretches (∼2690 cm^{-1}) are excited. For concentrations ≤2.5 mol %, alcohol monomers dominate the pump−probe signals, and all three alcohols yield monoexponential decays with decay times of ∼2 ps (varying somewhat for the different alcohols). In the 5 mol % samples studied, molecules associated with oligomers dominate the signals. The signals decay to negative values (increased absorption), but the rates of the vibrational excited state decays are unchanged from those observed in the 2.5 mol % samples. The negative signals recover on two time scales. We propose a model in which hydrogen bond dissociation, following vibrational relaxation, increases the concentration of non-hydrogen-bond donating hydroxyl groups and produces the observed negative signal. The observation of the same decay rates with and without hydrogen bond dissociation indicates that hydrogen bond breaking does not involve a new OD stretch relaxation pathway. Using a set of kinetic equations, the time constants for hydrogen bond dissociation and reformation have been determined to be 2−3 ps for breaking and roughly 20 ps and >10 ns for reformation. The fast recovering component of the negative signal reflects hydrogen bond reformation to an extent determined by a new local equilibrium temperature within the laser excitation volume. The slow recovering component reflects the slow diffusion of thermal energy out of the laser excitation volume.

I. Introduction

The physical and chemical properties of hydrogen bond network forming liquids reflect the extended intermolecular structures that result from hydrogen bond formation.[1,2] Hydrogen bonding not only influences the thermodynamic properties of liquids but also the dynamic properties because of the continual rupture and reformation of hydrogen bonds. Understanding these dynamics provides an intrinsically interesting step in the investigation of hydrogen bonding in chemical and biological processes. In this paper, we examine vibrational relaxation and hydrogen bond breaking using ultrafast infrared pump−probe experiments. The experiments are conducted on hydrogen bonded oligomers of alcohols in CCl_4 because at low concentration monomer vibrational dynamics can be studied, whereas at higher concentrations, oligomer vibrational dynamics and hydrogen bond breaking can be studied.

Experiments on hydroxyl vibrations excited by an IR laser and subsequent hydrogen bond breaking can have direct bearing on the thermal dynamics of hydrogen-bonded systems. In these experiments, we study OD stretches but consider the more common OH stretch of methanol. The stretching frequency is ∼3350 cm^{-1}. Thus, about one in 10^7 OH's in a pure methanol sample is excited at room temperature. In a sample that is 1 mL in volume, at any given time, there are $\sim 10^{15}$ excited OH stretches. The energy in such a stretch is sufficient to break a hydrogen bond. Although the experimental literature clearly indicates that vibrational relaxation can lead to hydrogen bond dissociation,[3−10] the question remains by what manner does vibrational relaxation of hydroxyl stretches lead to hydrogen-bond breaking?

The extent and strength of the hydrogen bonds in which a hydroxyl group participates greatly influences its stretching frequency and line width.[2] For a low concentration of alcohol dissolved in CCl_4, a relatively narrow monomer peak is observed at ∼2690 cm^{-1}, as shown in Figure 1.[4,11−14] When the concentration increases sufficiently, oligomers form. Oligomers that are not rings have two terminal alcohols. Each of these participates in only one hydrogen bond. On one end, the hydroxyl donates, but does not accept, a hydrogen bond. The other end accepts, but does not donate, a hydrogen bond. The nondonating hydroxyl is not shifted in frequency from the monomer. At low concentration of alcohol in CCl_4, monomers dominate the 2690 cm^{-1} peak, whereas at sufficiently high alcohol concentration, the terminal alcohol that does not donate a hydrogen bond dominates the 2690 cm^{-1} peak.[13] Therefore, by changing the alcohol concentration, ultrafast IR pump−probe experiments can be conducted on either monomers or on alcohols that accept, but do not donate a hydrogen bond. Comparisons of these experiments permit us to observe how the formation of hydrogen bonds influences the dynamics following vibrational excitation. Experimental studies of vibrational relaxation in hydrogen bonded liquids frequently invoke hydrogen bond dissociation following vibrational excitation to explain the observed experimental results.[3−10] One commonly proposed mechanism for this bond dissociation involves the relaxation of the high frequency hydroxyl stretch directly into the intermolecular hydrogen bond coordinate causing the rupture of a hydrogen bond.[3,4,6,15] This represents a predissociative mechanism for vibrational relaxation and hydrogen bond rupture. Alternatively, the initial relaxation of the hydroxyl stretch could involve the excitation of other intramolecular vibrations of the

* To whom correspondence should be addressed.

10.1021/jp021170w CCC: $22.00
Published on Web 09/17/2002

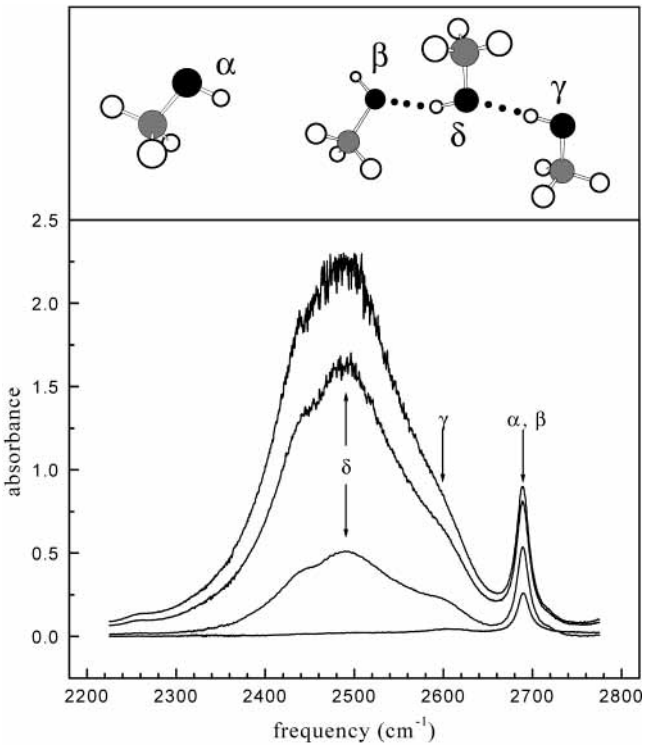

Figure 1. Steady-state IR spectrum of methanol-*d* in CCl_4 as a function of concentration in mol %. Concentrations of 1.0, 2.5, 3.8, and 5 mol % appear from bottom to top. α refers to isolated monomeric molecules, β refers to ODs that accept, but do not donate, hydrogen bonds, γ refers to molecules that donate, but do not accept, hydrogen bonds, and δ refers to molecules that donate and accept hydrogen bonds. The drawing of a monomer and a trimer show the different types of hydroxyl groups with the appropriate labels.

same molecule and subsequent hydrogen bond breaking.[16,17] This represents a sequential relaxation mechanism, where hydrogen bond dissociation would be a secondary relaxation event. By exciting a hydroxyl stretch that does not donate a hydrogen bond, the predissociation mechanism of vibrational relaxation can be eliminated and the rate and efficiency of sequential hydrogen bond dissociation can be investigated.

As demonstrated by Levinger et al. for methanol-*d* dissolved in CCl_4,[17] excitation of an OD stretch where the deuterium does not participate in a hydrogen bond still leads to the fast dissociation of hydrogen bonds. The present investigation has extended this study to ethanol-*d* and 1-propanol-*d* in CCl_4 and observed the same qualitative features. The 2.5 mol % samples of all three alcohols have signals that decay on the 2 ps time scale. This provides a measure of the $\nu = 1$ excited state lifetime of the OD stretch. Although the initial decay still occurs on the 2 ps time scale for the 5 mol % samples, the signal decays to a negative value corresponding to an increased absorption. This negative going signal subsequently decays on a 20 ps time scale and a >10 ns time scale. As will be discussed, the increased absorption results from the transient dissociation of hydrogen bonds. The hydrogen bond dissociation follows vibrational relaxation and occurs with a 2−3 ps time constant. This represents the rate with which energy transfers from the intra- to the intermolecular hydrogen bond degrees of freedom. The subsequent decay of the increased absorption reflects the time scale for energy flow out of the initially excited oligomers and hydrogen bond recombination. The extent and rate of the decay are determined by the time evolution of the vibrational occupation numbers and the approach to a new elevated equilibrium temperature. The increased temperature is caused by the deposition of the optical energy in the sample. The small increase in sample temperature following vibrational relaxation causes an increase in the number of non-hydrogen-bond donating molecules. This change in temperature decays on a millisecond time scale, before the next pump pulse arrives at the sample, but not in the 300 ps time scale of the pump−probe experiment.

II. Experimental Methodology

Deuterated methanol-*d*, ethanol-*d*, 1-propanol-*d* (Aldrich, 99.5+ atom %), and carbon tetrachloride (Aldrich, HPLC grade) were used as received. These molecules have deuterated hydroxyl groups and protonated alkyl groups. Samples were prepared by weight at 2.5 and 5 mol %. Previous experiments examining more concentrations demonstrated that these are critical concentrations.[17] Spectroscopic measurements used home-built copper cells with CaF_2 windows. Teflon spacers of 1 and 2 mm yielded absorbances in the range of 0.5−1.2, respectively, for the non-hydrogen-bond donating peak at ∼2690 cm^{-1} for all solutions studied. In these sample cells, the solution came in contact only with the CaF_2 and Teflon, because metals such as copper catalyze the decomposition of alcohols in CCl_4 solution.[18]

The laser system used in these experiments consists of a home-built Ti:sapphire oscillator and regenerative amplifier whose output pumps a three-stage optical parametric amplifier (OPA) designed and built in house to produce tunable mid-infrared light.[17] A bandwidth limiting slit in the stretcher determines the bandwidth of the amplified seed pulse and provides control of the IR pulse duration. Given the reduced bandwidth, care was taken to ensure that the stretching was sufficient to avoid high peak power damage in the regenerative amplifier. The slit in the stretcher produces temporal wings in the output of the regenerative amplifier. However, the four nonlinear processes in the OPA eliminate the wings in the IR pulse. The IR pulse duration was measured by autocorrelation. The pulses have Gaussian profiles in time and frequency with fwhm of 200 fs in time and 80 cm^{-1} in frequency. The time-bandwidth product was always between 1 and 1.2 times the transform limit of 0.44. The IR output is 1−2 μJ per pulse centered at 2690 cm^{-1}.

The mid-IR pulses are split into pump (90%) and probe (10%) beams that traverse different paths before crossing in the sample. The pump beam is chopped at 500 Hz and directed along a variable path length delay line. A ZnSe Brewster-plate polarizer is used to set the probe beam polarization. A small amount of the mid-IR light is split off and used for shot-to-shot normalization. Signal and reference beams impinge on matched liquid-nitrogen-cooled MCT detectors whose outputs are processed by identical gated integrators, divided by an analogue processor, and input to a lock-in amplifier. A computer collects the output of the lock-in with an A/D board.

III. Steady-State Infrared Spectral Analysis

The steady-state infrared absorption spectrum of methanol-*d* dissolved in CCl_4 is shown in Figure 1. Similar spectra have been collected for ethanol-*d* and 1-propanol-*d*. At low concentrations, alcohol monomers, termed α absorbers, dominate the spectrum.[11−13] These species have an absorption maximum at ∼2690 cm^{-1}. As the concentration increases, the alcohols begin to aggregate, forming ring- and chainlike oligomer structures.[19,20] For the hydrogen bonded chains, the terminal alcohols have distinct OD stretch absorption frequencies and line shapes when compared to the alcohols present in the middle of a chain.[11−13]

TABLE 1: Approximate Fractional Populations Extracted from FTIR Spectra for Methanol-*d* in CCl_4

conc (mol %)	β/α	α	β	γ	δ
1.0	0.10	0.82	0.08	0.08	0.02
2.6	0.36	0.44	0.16	0.16	0.24
3.7	1.0	0.20	0.20	0.20	0.39
5.1	1.4	0.15	0.21	0.21	0.43

The terminal alcohol that receives a hydrogen bond but does not donate a hydrogen bond, termed a β absorber, has an OD stretch absorption frequency that cannot be distinguished from the α absorbers. The terminal alcohol that donates a hydrogen bond but does not accept one, termed a γ absorber, has an OD stretch frequency shifted by 100 cm^{-1} to $\sim$260 cm^{-1} and a significantly broader line shape. Alcohol molecules that both receive and donate hydrogen bonds, termed δ absorbers, have a broad OD stretch spectrum, centered at $\sim$2490 cm^{-1}. The experiments presented in this article excited the α/β peak of methanol-*d* at 2690 cm^{-1}. For ethanol-*d* and 1-propanol-*d*, the α/β peaks are centered at 2685 cm^{-1}.

The equilibrium populations of these different hydrogen bonding configurations can be determined by analyzing the infrared spectrum. The areas of the peaks, normalized by the relative extinction coefficients of 1:3.5:10 for the α/β:γ:δ absorbers,[21] respectively, provide the relative populations of the α/β, γ, and δ species as a function of concentration. Further analysis provides the relative contributions of the α and the β species to the α/β peak. Because of the low probability of alcohol molecules participating in three hydrogen bonds, very little branching occurs in the hydrogen bonded chains and rings formed by alcohols.[19,22,23] For an unbranched chain, there will be one β for every γ, whereas for an unbranched ring there will be neither a β nor a γ. This leads to a β concentration that equals the γ concentration, with the rest of the α/β peak intensity originating from alcohol monomers.

Using the above relationships, an analysis has been conducted for methanol-*d* in CCl_4, and the results appear in Table 1. The largest change in the β:α concentration ratio occurs when the concentration increases from 2.5 to 3.7 mol %, which also corresponds to the concentration change that leads to the onset of appreciable hydrogen bond dissociation following α/β vibrational excitation.[17]

IV. Time Dependent Experimental Results

Pump−probe data for excitation of non-hydrogen-bonded OD stretches appear in Figures 2−4. Figure 2 shows the decay of the excited OD stretch for 2.5 mol % ethanol-*d* and 1-propanol-*d*. The data for the 2.5% methanol-*d* has been published previously.[17] These data were taken with the probe polarization parallel to the pump polarization. Orientational diffusion is sufficiently slow that it does not contribute to the decays. At short delays, a nonresonant signal originating from the CCl_4 solvent strongly influences the signal.[17] The time dependence of the nonresonant signal was determined by measuring the signal in neat CCl_4. These experiments demonstrate that the solvent signal only contributes to the total signal for delay times of less than 1 ps. The nonresonant signal cannot be simply subtracted from the resonant signal because, when both are present, there will be cross terms at the polarization level. Consequently, time delays $\leq$1 ps will not be utilized in the analysis of the vibrational dynamics.

As previously observed for 2.5 mol % methanol-*d*,[17] the pump−probe signal undergoes a single-exponential decay for all three alcohols. The decay times of 2.04 $\pm$ 0.07 ps for ethanol-*d* and 2.45 $\pm$ 0.07 ps for 1-propanol-*d* provide the vibrational lifetime of the non-hydrogen-bonded OD stretch. These times are quite close to the 2.15 $\pm$ 0.07 ps lifetime of the non-hydrogen-bonded OD stretch in methanol-*d*.[17] The short lifetimes indicate that the free OD stretching vibration strongly couples to other modes in the system, resulting in the rapid redistribution of the initial excitation energy to a number of intra- and intermolecular vibrations. Vibrational relaxation can occur through a combination of intramolecular and intermolecular pathways.[24] CCl_4 has low-frequency internal modes and provides a continuum of bulk solvent modes that extend to $\sim$150 cm^{-1}.[25] A likely path for vibrational relaxation of the OD stretch involves the population of a number of other intramolecular modes of the absorbing molecule and one or more modes of the CCl_4 solvent continuum to satisfy energy conservation. Dlott and co-workers have recently demonstrated that vibrational relaxation of the hydroxyl stretch of methanol and other alcohols results in the excitation of internal modes in the alcohols.[16,26]

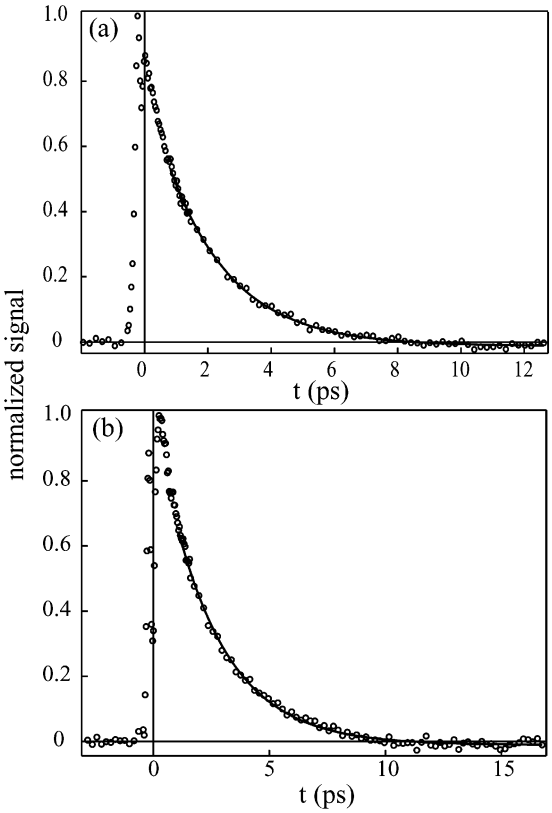

Figure 2. Pump−probe signal for 2.5 mol % samples of (a) ethanol-*d* and (b) 1-propanol-*d* in CCl_4. The data for methanol-*d* has been published previously.[17] All three decays are single exponentials yielding vibrational lifetimes of 2.15, 2.04, and 2.45 ps, for methanol-*d*, ethanol-*d*, and 1-propanol-*d*, respectively.

These relaxation rates (1/decay time) exceed those measured by Laenen et al. for non-hydrogen-bonded OH stretch decays of methanol and ethanol.[27,28] It is possible that the difference lies in the deuteration of the MeOD molecule. The sum of the ν_6 methyl rock (1232 cm^{-1}) and the ν_5 valence angle deformation (1467/1447 cm^{-1}) could provide a resonant intramolecular pathway for the vibrational relaxation of the OD stretch that is not available to an OH stretch.[29] Indeed, an ab initio calculation of the vibrational modes in methanol and its deuterated isotopomers showed significant Fermi interaction between the OD stretch and the $\nu_5 + \nu_6$ combination.[30] No Fermi interaction is observed for protonated methanol.

The pump−probe signal for 5 mol % samples of all three alcohols studied differ significantly from those of the 2.5 mol

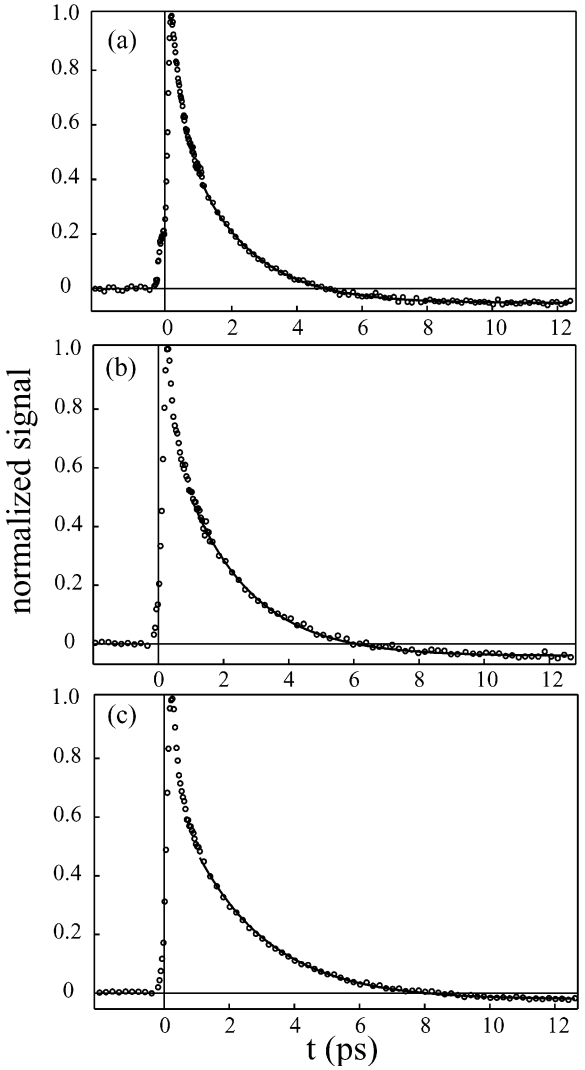

Figure 3. Short time pump−probe data for 5 mol % samples of (a) methanol-*d*, (b) ethanol-*d*, and (c) 1-propanol-*d* in CCl_4. The solid lines show the fits to the kinetic equations, and the open circles show the data points for delay times up to 13 ps.

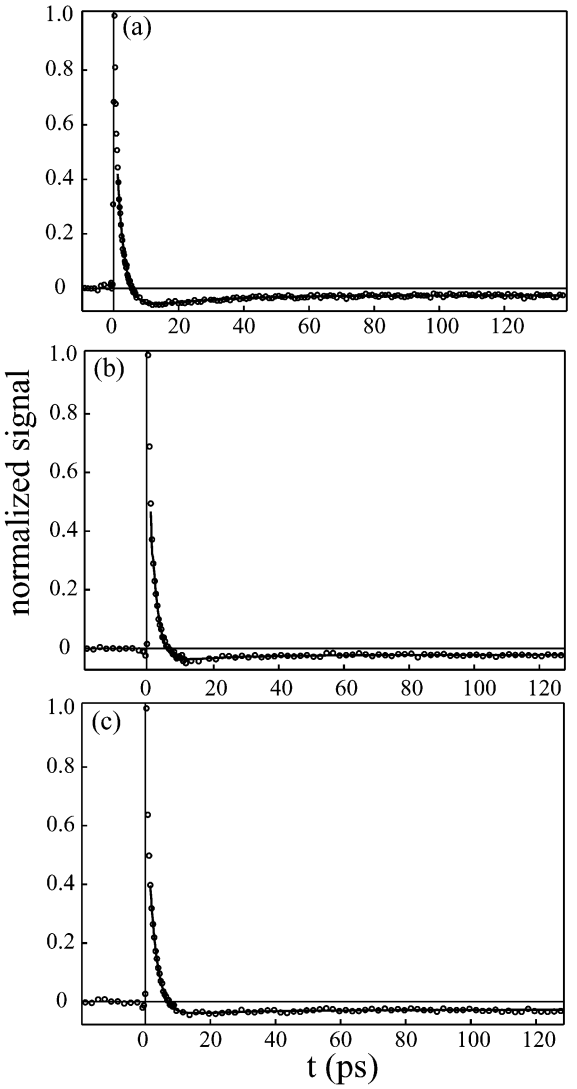

Figure 4. Long time pump−probe signal for 5 mol % samples of (a) methanol-*d*, (b) ethanol-*d*, and (c) 1-propanol-*d* in CCl_4. The solid lines show the fits to the kinetic equations, and the open circles show the data points for delay times up to 130 ps.

% samples, as displayed in Figures 3 and 4. Figure 3 shows the short time behavior out to a delay time of 13 ps. Figure 4 shows the long time behavior out to a delay time of 130 ps. These data were taken with the probe polarization rotated by 54.7° from the pump polarization. At this angle, often termed the magic angle, the diffusive orientational relaxation does not cause the signal to decay.[31] Initially, the signal decays to a negative, nonzero value. This occurs at the same rate as the vibrational decay observed for the 2.5 mol % samples. This negative signal then recovers on a time scale roughly an order of magnitude slower than the initial decay. A negative signal persists for delay times of up to 300 ps (not shown), the limit of the delay line. Fitting of the pump−probe signal indicates that the recovery of the persistent negative signal occurs with a time constant of >10 ns. The significance of these dynamics will be discussed in the following section, where a kinetic model is constructed to explain the pump−probe dynamics.

The possible contribution of γ and δ excitations to the dynamics observed in these experiments can be determined by calculating the overlap integrals for a laser bandwidth of 80 cm^{-1} and the widths and positions of the different peaks in the spectrum. For excitation at 2690 cm^{-1}, roughly 1% of the signal results from excitation of the γ and δ bands. For excitation at 2720 cm^{-1}, roughly 0.2% of the signal comes from the γ and δ bands. Pump−probe experiments were also conducted at 2720 cm^{-1} on a sample of 5 mol % methanol-*d*.[17] By shifting the wavelength to the blue, the overlap with the γ and δ bands is reduced. The decays were found to be indistinguishable, demonstrating that the negative signals observed in the pump−probe experiments do not result from the excitation of γ or δ absorbers.

V. Kinetic Model and Discussion

When the majority of alcohol molecules in solution are isolated monomers, the population decay of the OD stretch will be described by

$$\frac{dN_e(t)}{dt} = -k_r N_e(t) \tag{1}$$

where k_r is the rate for vibrational relaxation and $N_e(t)$ is the vibrationally excited monomer (α) concentration. Equation 1 has the solution

$$N_e(t) = N_e(0)e^{-k_r t} \tag{2}$$

As discussed in section III, analysis of the IR spectrum indicates

that the majority of alcohol molecules in 2.5 mol % solutions exist as monomers. Equation 2 accurately describes the signal of the 2.5 mol % samples for delay times in excess of 1 ps. At shorter delay times, the nonresonant CCl_4 signal interferes with the signal resulting from the resonant excitation of the OD stretch.[17]

The signals observed for the 5 mol % samples contain significantly more complex dynamics than the 2.5 mol % samples. The decay of the initially excited vibrations in the 5 mol % samples occurs with a similar rate as in the 2.5 mol % samples, but it leads to a signal with an increased absorption on a 2 ps time scale. The increased absorption, or alternatively the negative signal, subsequently decays on two time scales, one of ~20 ps and the other in excess of 10 ns. As will be discussed, the dissociation of hydrogen bonds following vibrational relaxation produces the increased complexity of the observed dynamics. The description of these dynamics requires a more complex kinetic model than eq 1 for the vibrational relaxation of monomers.

Consider an ensemble of vibrationally excited β ODs, which accept, but do not donate, a hydrogen bond. If vibrational relaxation leads to hydrogen bond breaking in some fraction of the ensemble, the dissociation of hydrogen bonds will lead to an increased population of α/β alcohols. Spectroscopically, this will result in increased α/β absorption at 2685−2690 cm^{-1} and a negative pump−probe signal. The manner in which hydrogen bond breaking leads to an increased α/β population can be pictured as follows. The dissociation of the hydrogen bond in a dimer will convert the β and γ absorbers of the dimer into two α absorbers. For dissociation of the hydrogen bond a β OD accepts in an oligomer, the β will become an α OD and the remaining oligomer will have a new β OD. If a hydrogen bond breaks somewhere else in the oligomer, the initial β will remain and another β will also be formed. In all cases, where initially one absorber contributes to the α/β peak, two absorbers will contribute to the absorption after hydrogen bond rupture. We attribute the negative going signals appearing in Figures 3 and 4 to an increased α/β peak absorption following hydrogen bond breakage and the decay of this increased absorption to the reformation of the transiently dissociated hydrogen bonds.

$N_e(t)$ represents the number of excited OD vibrations. These vibrationally excited molecules can be separated into three populations: those that return to the ground vibrational state and do not break hydrogen bonds, F_g, those that return to the ground state and break hydrogen bonds that reform quickly, F_f, and those that return to the ground state and break hydrogen bonds that reform slowly, F_s. The sum of these fractions equals unity. In contrast to the model used previously,[17] we do not assume hydrogen bond dissociation instantly follows vibrational relaxation; that is, we do not assume that the rate of hydrogen bond breaking following vibrational relaxation greatly exceeds the rate of vibrational relaxation. Those molecules that proceed to dissociate hydrogen bonds will reside temporarily in a configuration that cannot be distinguished experimentally from those vibrationally relaxed molecules that do not lead to hydrogen bond breaking. These intermediate populations, N^*_{gf} for molecules that quickly reform hydrogen bonds and N^*_{gs} for those that slowly reform hydrogen bonds, decay with the hydrogen bond breaking rate, k_b. The subensemble of molecules that result from the dissociation of the hydrogen bonds can be observed experimentally and will be represented by N_{gf} for molecules that reform hydrogen bonds quickly and N_{gs} for molecules that reform hydrogen bonds slowly. The populations N_{gf} and N_{gs} will finally decay to the ground state N_g with the hydrogen bond reformation rates, k_f for N_{gf} and k_s for N_{gs}. The detailed population dynamics can be represented by the following differential equations:

$$\frac{dN^*_{gf}(t)}{dt} = F_f k_r N_e(t) - k_b N^*_{gf}(t) \tag{3}$$

$$\frac{dN^*_{gs}(t)}{dt} = F_s k_r N_e(t) - k_b N^*_{gs}(t) \tag{4}$$

$$\frac{dN_{gf}(t)}{dt} = k_b N^*_{gf}(t) - k_f N_{gf}(t) \tag{5}$$

$$\frac{dN_{gs}(t)}{dt} = k_b N^*_{gs}(t) - k_s N_{gs}(t) \tag{6}$$

$$\frac{dN_g(t)}{dt} = F_g k_r N_e(t) + k_f N_{gf}(t) + k_s N_{gs}(t) \tag{7}$$

where the observed signal equals

$$S(t) = 2N_e(t) - N_{gf}(t) - N_{gs}(t) \tag{8}$$

The factor of 2 in front of the first term on the right-hand side reflects the equal contributions of the reduced ground-state absorption and the stimulated emission to the pump−probe signal that arise from vibrationally excited molecules. The second and third terms do not have a factor of 2 because increases in the α and β populations will only change the ground-state absorption; there is no stimulated emission contribution. The solution of these differential equations results in the following expression for the pump−probe signal:

$$\begin{aligned} S(t) = {} & 2Q(N_e(0)e^{-k_r t}) - \\ & Q\left(\frac{F_f N_e(0) k_r k_b}{(k_b - k_f)(k_f - k_r)(k_b - k_r)}\right)\{(k_b - k_f)e^{-k_r t} + (k_f - \\ & k_r)e^{-k_b t} - (k_b - k_r)e^{-k_f t}\} - Q\left(\frac{F_s N_e(0) k_r k_b}{(k_b - k_s)(k_s - k_r)(k_b - k_r)}\right) \\ & \{(k_b - k_s)e^{-k_r t} + (k_s - k_r)e^{-k_b t} - (k_b - k_r)e^{-k_s t}\} \end{aligned} \tag{9}$$

where Q is a normalization parameter.

The expression for the pump−probe signal, as represented by eq 9, differs from the one used in the initial investigation of β OD dynamics in methanol-*d* clusters in CCl_4.[17] As mentioned above, the previous work assumed the rate of hydrogen bond breaking to be much faster than the rate of vibrational relaxation, a limit that can be achieved by letting $k_b \rightarrow \infty$ in eq 9. Although this assumption provided quality fits to the experimental data, further statistical analysis demonstrated that treating the hydrogen bond breaking rate as an adjustable parameter leads to higher quality fits and provides information on the magnitude of k_b.

The fits of eq 9 to the data appear in Figures 3 and 4, whereas the parameters extracted from the fits appear in Table 2. The dynamics observed for all three alcohols strongly resemble one another, with one important exception. The fraction of excited molecules that proceeded to break and then reform hydrogen bonds quickly, F_f, decreases with increasing alkyl chain length. F_s does not exhibit an alkyl chain length dependence. A potential explanation will be discussed shortly. The rate of vibrational relaxation, within experimental error, does not change with concentration, as observed in the previous

TABLE 2: Parameters Extracted from Fit to Eq 9 for 5 Mol % Data

	F_f	F_s	k_r^{-1} (ps)	k_b^{-1} (ps)	k_f^{-1} (ps)	k_s^{-1} (ns)
methanol-*d*	0.13 ± 0.04	0.06 ± 0.01	2.15 ± 0.07[a]	2.5 ± 1	23 ± 8	>10
ethanol-*d*	0.07 ± 0.03	0.06 ± 0.01	2.04 ± 0.07[a]	2 ± 1	18 ± 6	>10
1-propanol-*d*	0.04 ± 0.01	0.06 ± 0.01	2.45 ± 0.07[a]		20 ± 6	>10

[a] Fixed at value determined from 2.5 mol % samples.

study of methanol-*d* in CCl_4.[17] Consistent with this observation, we fix k_r to the values measured for the 2.5 mol % samples. The hydrogen bond dissociation time constant has been determined for both methanol-*d* and ethanol-*d* to be 2−3 ps. For 1-propanol-*d*, k_b could not be obtained from the fits because of the smaller fraction of excited molecules that proceeded to break hydrogen bonds. The hydrogen bond reformation time constants have been determined to be roughly the same for all three alcohols, with $k_f^{-1} \approx 20$ ps and $k_s^{-1} > 10$ ns.

With these results, a mechanism for the underlying dynamics can be constructed. The relaxation rate, k_r, does not depend on the extent of hydrogen bond dissociation observed experimentally. This fact strongly suggests that an additional vibrational relaxation channel does not emerge as the alcohol concentration increases to produce oligomers. For a fraction of the excited molecules, vibrational relaxation leads to hydrogen bond breaking. The experimental data indicate that these events occur sequentially, with hydrogen bond dissociation time constants of $k_b^{-1} = 2.5 \pm 1$ ps and $k_b^{-1} = 2 \pm 1$ ps for methanol-*d* and ethanol-*d*, respectively. Following the vibrational relaxation of the OD stretch, the initially excited alcohol molecule is vibrationally "hot". The molecule is not yet in thermal equilibrium. Rather, some set of specific modes is excited.[26] These modes will include modes that involve the oxygen atom, which is the hydrogen bond acceptor on the initially excited β OD. The locally hot nonequilibrium vibrational distribution will transfer vibrational energy from the intramolecular vibrations of the initially excited molecule to the intermolecular hydrogen bonding network, leading to hydrogen bond breaking. The rates of thermal hydrogen bond dissociation have been widely studied using MD simulations, and it is interesting to compare these with our experimental findings. Extensive MD simulations of liquid methanol at 300 and 200 K have been performed.[22] The simulations gave a mean H-bond lifetime of 5−7 ps at 300 K increasing by approximately an order of magnitude at 200 K. These numbers agree with NMR data.[32] Molecular dynamics simulations on a solution of 10% methanol in CCl_4 suggest that the time scale for room temperature thermal hydrogen bond breaking is 46 ps and decreases as the concentration of methanol increases.[19] In the MD simulations, the time is defined as that required for a particular hydrogen bonded methanol to form a new hydrogen bond with a different partner. The time for breaking a hydrogen bond and reforming a hydrogen bond including reforming the bond with the same partner is faster. The MD simulations determine this time to be 2 ps independent of the methanol concentration in the CCl_4 solution.[19]

Vibrational excitation increases the local vibrational energy content of the hydrogen bonded network, resulting in faster hydrogen bond breaking than under room temperature thermal equilibrium conditions. The experimental observable discussed in this paper is sensitive to broken hydrogen bonds that produce additional β species, giving rise to the negative going signal. Recombination that reduces the number of β's (or α's), whether with the initial partner or a different partner, will contribute to the decay of the negative signal. The similarity between k_b^{-1} determined experimentally in this study and the results of the molecular dynamics simulation is almost certainly fortuitous.

The energy transfer from intra- to intermolecular degrees of freedom does not result in the full equilibration of the sample. Given the bulk sample temperature, too many hydrogen bonds are broken. The hot hydrogen bond network further relaxes. This relaxation occurs on two time scales, $k_f^{-1} \approx 20$ ps and $k_s^{-1} > 10$ ns, with time constants that vary little from one alcohol to another. The small variation in fast recombination rates for the different alcohols studied suggests that the time scale observed does not represent the time for oligomer reorganization, because mechanical[33,34] and dielectric[35] reorganization dynamics of methanol, ethanol, and 1-propanol differ significantly. Alternatively, these dynamics could involve the time for CCl_4 reorganization or the time for energy transfer from the hydrogen bonded oligomers to the CCl_4 solvent. The fast hydrogen bond reformation rates resemble the rate of energy transfer from methanol to CCl_4 observed by Iwaki and Dlott.[16] In the experiments of Iwaki and Dlott on a 75 mol % methanol 25 mol % CCl_4 sample, the increase in the anti-Stokes Raman signal from CCl_4 following the vibrational excitation of the OH stretch of methanol was complete within 50 ps, which provides a measure of the local thermal equilibration time. Then, it is reasonable to assume that the fast relaxation involves equilibration of the nonequilibrium distribution of vibrations and the flow of vibrational energy out of the initially excited oligomer into the CCl_4 solvent. Approximately 1 in 1000 oligomers is initially excited. As energy leaves the initially excited oligomers and spreads through the solvent, the local temperature decreases, leading to the reformation of hydrogen bonds. Approximate calculations based on the rate of thermal diffusion in CCl_4 show that the time scale for macroscopic thermal equilibration within the laser spot occurs on the order of 100 ps, consistent with the time for the completion of the observed fast recovery of the negative signal.

Within this picture, the slowly recovering offset results from the finite temperature change within the volume of vibrational excitation by the laser. The equilibrium properties of the hydrogen bonded oligomers in CCl_4 have significant temperature dependence as can be seen in Figure 5, the steady-state temperature dependent difference spectrum that results from a 7 K temperature increase from 294 to 301 K. The energy absorbed in the pump−probe experiment will cause the sample temperature to increase. Detailed calculations indicate that the temperature rise associated with the absorption of IR photons once equilibration has occurred in the laser irradiated spot is ~0.01 K. This temperature rise, although very small, will leave the system with more broken hydrogen bonds and, therefore, more absorption at the α/β peak frequency than before laser irradiation. Careful temperature-dependent measurements of the absorption spectrum and calibration of the pump−probe instrument shows that the experiment is sensitive to the change in hydrogen bonding associated with a ~0.01 K temperature change. The temperature rise will decay by thermal diffusion out of the laser irradiated spot, which is very long compared to the maximum delay in the experiments, 300 ps. Therefore, the slow component does not appear to decay at all. In a previous publication studying only methanol-*d*,[17] the long time scale decay was attributed to nongeminate recombination. It now

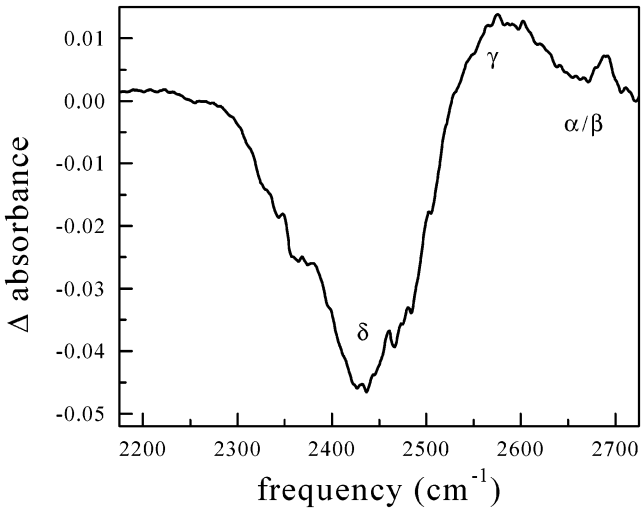

Figure 5. Temperature dependent difference spectrum for 26 mol % methanol-*d* in CCl_4. The plot shows the change in absorbance for the 294 K spectrum subtracted from the 301 K spectrum. Positive changes in absorbance will result in a negative pump−probe signal. The α, β, and γ increased absorbance and the δ decreased absorbance result from a reduced equilibrium number of hydrogen bonds. A simple calculation based on the heat capacity of the solutions studied and the laser energy deposited per unit volume predicts a temperature change on the order of 0.01 K. This produces a change in absorbance for the α/β peak of the same order as that of the negative offsets in the pump−probe experiments.

seems clear that the long time scale decay is governed by thermal diffusion.

Attributing the long time negative offset to a temperature change provides further support for assigning the faster recombination rate, k_f, to be the local equilibration rate, because it provides the rate with which the sample approaches local thermal equilibrium. The influence of a finite temperature change following excitation of the hydroxyl stretch in hydrogen bonded liquids has been observed by Laenen et al.,[9] as well as Lock et al.[7] In all cases, the average number of hydrogen bonds in the solution decreases with increasing temperature, resulting in an increased population of alcohol molecules that do not participate in two hydrogen bonds, namely, α, β, and γ species.

The similarity in the magnitudes for the long time offsets for all three alcohols studied can also be explained within this context. The solutions made with all three alcohols have very similar concentrations and extinction coefficients. This results in very similar quantities of energy being deposited per unit volume for all three alcohols. Because the heat capacities of the solutions also vary little due to the dominant contribution of the CCl_4 solvent to the solution heat capacity, all three samples should have similar thermal offsets, as observed experimentally. This holds true when the offsets are reported as a fraction of the normalized signal, even for variable laser powers, because both the signal and the change in temperature depend linearly on the energy absorbed.

However, the magnitude of the negative signal that decays from the local hydrogen bond recovery does depend significantly on the alcohol being studied, with F_f for methanol-*d* being a factor of 3 larger than F_f for 1-propanol-*d*. This variation may reflect the increased number of vibrational degrees of freedom for each molecule excited as the size of the alcohol increases. 1-Propanol has 30 vibrational degrees of freedom, whereas methanol has only 12. If the first step in the vibrational relaxation of the OD stretch involves intramolecular vibrational redistribution, a larger molecule will be able to accommodate a greater internal energy, leaving less energy associated with the modes that can couple into the hydrogen bond intermolecular degrees of freedom to produce dissociation of hydrogen bonds.

VI. Concluding Remarks

The dynamics of OD stretch vibrational relaxation have been investigated for methanol-*d*, ethanol-*d*, and 1-propanol-*d* dissolved in CCl_4. The studies involved excitation of non-hydrogen-bond donating OD stretches. For 2.5 mol % solutions, the pump−probe experiment predominantly excites free monomers. Under these circumstances, the signals have single exponential decays that provide the lifetime of the OD stretch vibration. The alcohols studied have lifetimes of 2.15, 2.04, and 2.45 ps for methanol-*d*, ethanol-*d*, and 1-propanol-*d*, respectively. For the 5 mol % samples studied, excitation of the OD stretch leads to hydrogen bond dissociation. The initial vibrational relaxation occurs with the same time constants as the 2.5 mol % samples, so the onset of hydrogen bond dissociation does not appear to result from a new vibrational relaxation channel. Following vibrational relaxation, hydrogen bond breaking occurs with a 2−3 ps time constant. A similar time scale for sequential hydrogen bond breaking has also been observed for excitation of methanol-*d* molecules that both accept and donate hydrogen bonds.[36]

The dynamics of hydrogen bond reformation have also been determined. The hydrogen bond reformation occurs on two time scales for all three alcohols studied, a fast recovery with a time constant of ~20 ps and a slow recovery with a time constant >10 ns. The slower recovery results in a long time negative offset in the pump−probe signal. The finite temperature increase resulting from the absorption of energy from the laser pulses produces the negative offset. The fast recombination occurring on the 20 ps time scale represents the time scale for equilibration to the new equilibrium temperature.

These dynamics can be utilized to construct a mechanistic picture for energy transfer in these systems. Initially, the energy deposited in the OD stretch undergoes intramolecular vibrational redistribution. This determines the vibrational excited-state lifetime of ~2 ps. Following intramolecular vibrational redistribution, energy transfers from intra- to intermolecular degrees of freedom. The 2−3 ps time scale for hydrogen-bond breaking indicates the rate of energy transfer and hydrogen-bond breaking. Energy then transfers from the alcohol oligomers into the CCl_4 solvent, a conclusion supported by the experiments of Iwaki and Dlott.[16] This step in the equilibration process proceeds on the 20 ps time scale. Because of the absorption of laser energy by the sample, the solution will equilibrate at an elevated temperature, resulting in the long-lived negative offset in the pump−probe signal. Between pump pulses, this offset will decay on the time scale of thermal diffusion in CCl_4.

These studies demonstrate that hydrogen bond breaking can occur following vibrational excitation of a non-hydrogen-bonded OD stretch. Because the excited OD stretch is not a hydrogen-bond donor, hydrogen-bond dissociation cannot occur by direct relaxation of the OD stretch into the hydrogen bond OD···O mode. Rather, the hydrogen-bond breaking is sequential. This sequential hydrogen-bond breaking mechanism appears to involve both a significant and fast route for energy relaxation in the hydrogen-bonded systems studied and may prove to apply to a wide array of hydrogen-bonded systems.

Acknowledgment. We thank Professor Nancy E. Levinger, Colorado State University at Fort Collins, for her very useful input to this work. This work was supported by the Department

of Energy (Grant DE-FG03-84ER13251), the National Science Foundation (DMR-0088942), and the National Institutes of Health (1RO1-GM61137).

References and Notes

(1) Schuster, P.; Zundel, G.; Sandorfy, C. *The Hydrogen Bond. Recent developments in theory and experiments*; North-Holland: Amsterdam, 1976.
(2) Henri-Rousseau, O.; Blaise, P. *Adv. Chem. Phys.* **1998**, *103*, 1.
(3) Graener, H.; Ye, T. Q.; Laubereau, A. *J. Chem. Phys.* **1989**, *91*, 1043.
(4) Graener, H.; Ye, T. Q.; Laubereau, A. *J. Chem. Phys.* **1989**, *90*, 3413.
(5) Keutsch, F. N.; Saykally, R. J. *Proc. Natl. Acad. Sci. U.S.A.* **2001**, *98*, 10533.
(6) Woutersen, S.; Emmerichs, U.; Bakker, H. J. *J. Chem. Phys.* **1997**, *107*, 1483.
(7) Lock, A. J.; Woutersen, S.; Bakker, H. J. *J. Phys. Chem. A* **2001**, *105*, 1238.
(8) Laenen, R.; Rauscher, C.; Laubereau, A. *J. Phys. Chem. A* **1997**, *101*, 3201.
(9) Laenen, R.; Rauscher, C.; Laubereau, A. *Chem. Phys. Lett.* **1998**, *283*, 7.
(10) Laenen, R.; Gale, G. M.; Lascoux, N. *J. Phys. Chem. A* **1999**, *103*, 10708.
(11) Liddel, U.; Becker, E. D. *Spectrochim. Acta* **1957**, *10*, 70.
(12) Kristiansson, O. *J. Mol. Struct.* **1999**, *477*, 105.
(13) Symons, M. C. R.; Thomas, V. K. *J. Chem. Soc., Faraday Trans. 1* **1981**, *77*, 1883.
(14) Staib, A. *J. Chem. Phys.* **1998**, *108*, 4554.
(15) Staib, A.; Hynes, J. T. *Chem. Phys. Lett.* **1993**, *204*, 197.
(16) Iwaki, L. K.; Dlott, D. D. *J. Phys. Chem. A* **2000**, *104*, 9101.
(17) Levinger, N. E.; Davis, P. H.; Fayer, M. D. *J. Chem. Phys.* **2001**, *115*, 9352.
(18) Kuppers, J. R. *J. Electrochem. Soc.* **1978**, *125*, 97.
(19) Veldhuizen, R.; de Leeuw, S. W. *J. Chem. Phys.* **1996**, *105*, 2828.
(20) zum Buschenfelde, D. M.; Staib, A. *Chem. Phys.* **1998**, *236*, 253.
(21) Bertie, J. E.; Zhang, S. L. *Appl. Spectrosc.* **1994**, *48*, 176.
(22) Matsumoto, M.; Gubbins, K. E. *J. Chem. Phys.* **1990**, *93*, 1981.
(23) Saiz, L.; Padro, J. A.; Guardia, E. *J. Phys. Chem. B* **1997**, *101*, 78.
(24) Kenkre, V. M.; Tokmakoff, A.; Fayer, M. D. *J. Chem. Phys.* **1994**, *101*, 10618.
(25) Moore, P.; Tokmakoff, A.; Keyes, T.; Fayer, M. D. *J. Chem. Phys.* **1995**, *103*, 3325.
(26) Wang, Z.; Pakoulev, A.; Dlott, D. D. *Science* **2002**, accepted.
(27) Laenen, R.; Rauscher, C. *Chem. Phys. Lett.* **1997**, *274*, 63.
(28) Laenen, R.; Simeonidis, K. *Chem. Phys. Lett.* **1999**, *299*, 589.
(29) Bertie, J. E.; Zhang, S. L. *J. Mol. Struct.* **1997**, *413*−*414*, 333.
(30) Miani, A.; Hanninen, V.; Horn, M.; Halonen, L. *Mol. Phys.* **2000**, *98*, 1737.
(31) Berne, B. J.; Pecora, R. *Dynamic Light Scattering*; J. Wiley: New York, 1976.
(32) Göller, R.; Hertz, H. G.; Tutsch, R. *Pure. Appl. Chem.* **1972**, *32*, 149.
(33) Berg, M. *J. Phys. Chem. A* **1998**, *102*, 17.
(34) *CRC Handbook of Chemistry and Physics*, 51st ed.; CRC Press: Boca Raton, FL, 1970.
(35) Kindt, J. T.; Schmuttenmaer, C. A. *J. Phys. Chem.* **1996**, *100*, 10373.
(36) Gaffney, K. J.; Davis, P. H.; Piletic, I. R.; Levinger, N. E.; Fayer, M. D. *J. Phys. Chem. A* **2002**, submitted.